CHAPTER: 5

Synthesis and Characterization of Cobalt-free $SrFe_{0.8}Mo_{0.1}W_{0.1}O_3$ Perovskite Structured Cathode for SOFCs Applications

Chapter 5

5.1 Introduction

As discussed in Chapter 1, extensive efforts have recently been focused on development of SOFCs with reduced operating temperature to overcome the performance degradation and working life of the SOFCs. However, this approach noticeably deteriorates the electrochemical activity of the electrode materials as a result of increased polarization resistance corresponding to electrodes. Particularly, the reduction in cell performance happens due to swift increase of polarization resistance at cathode with reducing operating temperature. Thus the kinetics and transport processes of oxygen reduction reaction (ORR) at the cathode considerably decreases at lower working temperatures which requires high activation energy to overcome the kinetic barriers of this reaction [Bevilacqua et al., 2007, Song et al., 2011; De Souza et al., 1998; Su et al., 2008]. The development of advanced cathode materials with high performance of ORR is extremely essential for intermediate temperature (IT)-SOFCs. It is known that the materials with perovskite-like structure having good mixed oxide ions and electronic conduction (MIECs) properties can be potentially promising candidates as cathode materials for IT-SOFCs. The overall surface area of MIECs leads to enough catalytic activity for ORR on the cathode surface as well as reduces the area specific resistance (ASR) [Choi et al., 2014; Yao et al., 2018]. Among various perovskite cathode materials for IT-SOFCs, high electrochemical performance is exhibited by cobalt (Co) containing perovskite cathode materials such as $La_{0.6}Sr_{0.4}Co_{0.2}Fe_{0.8}O_{3-\delta}$ (LSCF) [Baqué et al., 2017], $Pr_{1-x}BaCo_2O_{5+\delta}$ [Kim et al., 2015], $Ba_{0.5}Sr_{0.5}Co_{0.8}Fe_{0.2}O_{3-\delta}$ (BSCF) [He et al., 2016], $PrBa_{0.5}Sr_{0.5}Co_{1.5}Fe_{0.5}O_{5+\delta}$ (PBSCF) [Choi etal., 2014], and $NdBa_{1-x}Co_2O_{5+\delta}$ [Kim et al., 2015]. However, Co-containing cathodes cause many other disadvantages such as high thermal expansion coefficient (TEC) resulting mismatch with common electrolytes, poor stability and compatibility with commonly used electrolytes. In this regard, Cobalt-free $SrFeO_3$ perovskite structured cathode material

has low TEC, high mixed ionic-electronic conductivities and better ORR catalytic activity [Hodges et al., 2000; Jiang et al., 2012]. In addition, the cubic structure provides three-dimensional oxygen movement paths and it shows excellent electrochemical properties below 800°C [Yao et al., 2018]. However, some disadvantages are also observed as well. The structural phase and defects in $SrFeO_3$ are influenced by the distribution of oxygen vacancies and it can undergo a structural phase transition from cubic perovskite structure to orthorhombic brownmillerite structure. The oxygen vacancy concentration in $SrFeO_3$ reduces at decreasing oxygen partial pressure or increasing temperature, as a result, the orthorhombic brownmillerite phase forms. This is accompanied by noticeable changes in volume at temperatures below 850°C, which causes decrease in electronic and ionic conductivities [Savinskaya et al., 2007, Yu et al., 2014]. To suppress the structural phase transition, the modification approach of partial replacement of Fe sites in $SrFeO_3$ with other elements such as Mo, Nb, W, Ga, Ti, Sc, Al etc. is done. This can help in stabilizing the stable cubic perovskite structure which has better charge transport properties in a wide temperature zone [Anikina et al., 2009; Waerenborgh et al., 2005; Patrakeev et al., 2006]. Furthermore, $SrFeO_3$ cubic structured perovskite oxides such as $SrFe_{0.95}Ti_{0.05}O_3$, $Bi_{0.5}Sr0.5FeO_3$, $SrFe_{0.9}Nb_{0.1}O_3$, and $SrFe_{0.9}Sb_{0.1}O_3$, had been revealed to have a good electrochemical activity as potential cathode materials for SOFCs. Until now, there is comparatively less information on the effect of subgroup VI elements substitution in strontium ferrites [Jiang et al., 2012, Ling et al., 2010, Yu et al., 2014]. Recently, Mo substitution has been studied to investigate the sinterability, thermal expansion, electrical properties and oxygen nonstoichiometry. The molybdenum ions exhibit higher valence state than iron ions and formation of oxygen defects results simultaneously via changing the iron oxidation states, which are responsible for better electrical properties and electrode

catalytic activity. In addition, at lower Mo-doping content, $SrFeO_3$ is appropriate as symmetrical SOFCs for both cathode and anode materials [Xiao et al., 2012]. Zhu et. al. [Zhu et al., 2017] have investigated that the increasing the concentration of W into $SrFeO_3$, decreases the electrical conduction properties of the dense cathode samples due to the formation of W^{oo}_{Fe} defects which impede the creation of Fe^{3+}-O-Fe^{4+} polarons and subsequently increases the average length of Fe-O bonds. Moreover, they synthesized $SrFe_{0.8}W_{0.2}O_3$-$Ce_{0.8}Sm_{0.2}O_{2-\delta}$ (SFW-SDC) composite cathodes and found that SFW-SDC cathode reveals the best catalytic activity toward oxygen reduction reaction with smallest ASR values, because of its significant conductivity, low TEC and proper sinterability. Furthermore, it has been recommended and experimentally established that an ABO_3 perovskite cathode having co-doping at A or B site can cause synergistic effects with respect to electrochemical and thermal properties. As we know that both Mo and W are under the same periodic table column having similar ionic radii (0.59 Å and 0.6 Å) comparable to Fe^{3+} (0.645 Å), for that reason, both Mo and W are appropriate as doping elements for cobalt–free $SrFeO_3$ cubic perovskite as cathode material. To the best of our knowledge, Mo and W co-doped $SrFeO_3$ as a cathode material for SOFCs has not been investigated yet. In this regard, the present chapter demonstrates the thermal, electrical and electrochemical properties of Mo and W co-doped $SrFe_{0.8}Mo_{0.1}W_{0.1}O_3$ Perovskite for cathode applications. The obtained results indicate that $SrFe_{0.8}Mo_{0.1}W_{0.1}O_3$ can be a better choice as cathode material for IT-SOFCs.

5.2 Experimental details

5.2.1 Sample preparation

Three compositions of Mo and W doped $SrFeO_3$ samples, (i) 10 mol% Mo and 10 mol% W co-doped $SrFe_{0.8}Mo_{0.1}W_{0.1}O_3$ (SFMW), (ii) 20 mol% W doped

$SrFe_{0.8}W_{0.2}O_3$ (SFW) and (iii) 20 mol% Mo doped $SrFe_{0.8}$ $Mo_{0.2}O_3$ (SFM) were synthesized by using an efficient high energy ball milling (RETSCH-PM 400, Germany) method. The starting precursors were Strontium carbonate [$SrCO_3$, Hi-media, 99.00%], Iron oxide [Fe_2O_3, Himedia, 99%), Molybdenum trioxide [MoO_3, Alfa-aesar, 99.5%), Tungstic acid [H_2WO_4, Hi-media, 99.90%], and ethanol (Loba) for the sample synthesis. The stoichiometric quantity of starting chemicals such as Strontium carbonate ($SrCO_3$), Iron oxide Fe_2O_3 Tungstic acid (H_2WO_4), Molybdenum oxide MoO_3, as per the particular composition were weighed mixed manually using mortar-pestle. The obtained mixtures of raw materials were shifted to zirconia made milling jars. The zirconia balls were employed as grinding medium. The zirconia ball to raw materials powder ratio was fixed at 10:1. The milling speed of mixture was set at 300 rpm for 16 h with breaking time in each minute of 30 seconds clock wise followed by rotation of 30 seconds anti-clock wise direction. The as synthesized product was collected from milling jar and then sample was dried at 80ºC for 12 h continuously on hot plate in order to remove volatile components. After that, final product was grinded by using agate mortar-pestle to obtain a fine powder. The as synthesized $SrFe_{0.8}Mo_{0.1}W_{0.1}O_3$ powder has been calcined for 10 h at 1200°C followed by crushing into fine powder by an agate mortar-pestle. For electrochemical studies, cylindrical disc pellets having a diameter 10 mm and thickness 2mm have been prepared using hydraulic press at optimized load of 70 MPa. The obtained pellets were afterward sintered for 10 h at 1200° C in SiC furnace. Further, for compatibility studies with the common electrolytes, samarium doped ceria (SDC) $Ce_{0.8}Sm_{0.2}O_{2-\delta}$ an oxide ion conductor electrolyte powder and $Ba_{0.8}Ce_{0.1}Sn_{0.1}O_3$ (BCS) proton ion conductor electrolyte were prepared by high energy ball milling method followed by calcination at 1000 °C for 4 h.

5.2.2 Characterizations

The phase purity of both the electrolyte and cathode materials was confirmed by powder X-ray diffraction. The room temperature powder X-ray diffraction (XRD) patterns of the powder samples were characterized by Rigaku X-ray diffractrometer (Miniflex 600, $CuK_{\alpha 1}$ λ= 1.5406 Å over the range $20^o \leq 2\theta \leq 120^o$ at step width of 0.02^o/s. The Rietveld structural analysis of XRD data was carried out by FullProf Suite. Surface morphology and elemental compositional analysis of the cathode samples were done by ZEISS-EVO18 scanning electron microscope (SEM). For the electrode polarization resistance (Rp) measurement, the impedance spectra of a cylindrical disc pellet sintered at 1200^oC for 10hr was recorded using KEYSIGHT-E4990A impedance analyzer in the temperature range 200^oC-700^oC over the frequency range 20 Hz to 5kHz under inert ambient condition. The thermal expansion measurements of electrode samples were examined by using high temperature X-ray diffraction (HT-XRD) data using high resolution, 9kW, Rigaku SmartLab, Powder diffractometer.

Further, to prepare the electrolyte supported symmetrical cell, SDC electrolyte pellets were sintered at 1500 ℃ for 4h. The electrolyte-supported symmetrical cell has been fabricated by coating the slurry made by using the prepared cathode material SFMW, on both the surfaces of the dense sintered SDC electrolyte pellets. The electrolyte-supported symmetrical cell was then fired at 1100ºC for 1hr. The values of area specific resistance (ASR) with temperature were measured from the impedance measurement data in air. Moreover, the microstructures at SFMW/SDC/SFMW interface of the symmetrical cell were examined by the scanning electron microscope (SEM).

5.3. Results and discussion

5.3.1 Phase structure

The XRD patterns of the $SrFe_{0.8}Mo_{0.1}W_{0.1}O_3$ cathode material calcined at various temperatures and time durations are shown Figure 5.1a. A pure cubic phase is obtained for calcination at 1200ºC for 10 h, as all the XRD profiles are seen to be singlet corresponding to the ideal perovskite structure. However, a very week impurity peak of iron oxide (Fe_2O_3 JCPDS card, no. 87-1164) marked with asterisk symbols (*) is present in the XRD patterns of other samples calcined for smaller time durations. Rietveld structure refinement of the pure $SrFe_{0.8}Mo_{0.1}W_{0.1}O_3$ sample using cubic structure with space group P*m-3m* gives very good fit of the XRD pattern, as presented in Figure 5.2b. As discussed earlier, the transition metals having high valence state (like W^{6+}) can stabilize the cubic structure by substituting for the ions on the B-site of the Perovskite oxides [Yao et al., 2019]. Hence, the cubic perovskite structure can stabilize steadily via substituting high valence state Ta and Mo for Fe in the sample. The structural parameters and agreement factors for $SrFe_{0.8}Mo_{0.1}W_{0.1}O_3$ obtained after Rietveld refinement are, a = 3.9234(1) Å, R_p = 8.52%, R_{wp} = 12.2% and χ^2 = 1.33, respectively. The low value of χ^2 further confirms the cubic structure for $SrFe_{0.8}Mo_{0.1}W_{0.1}O_3$.

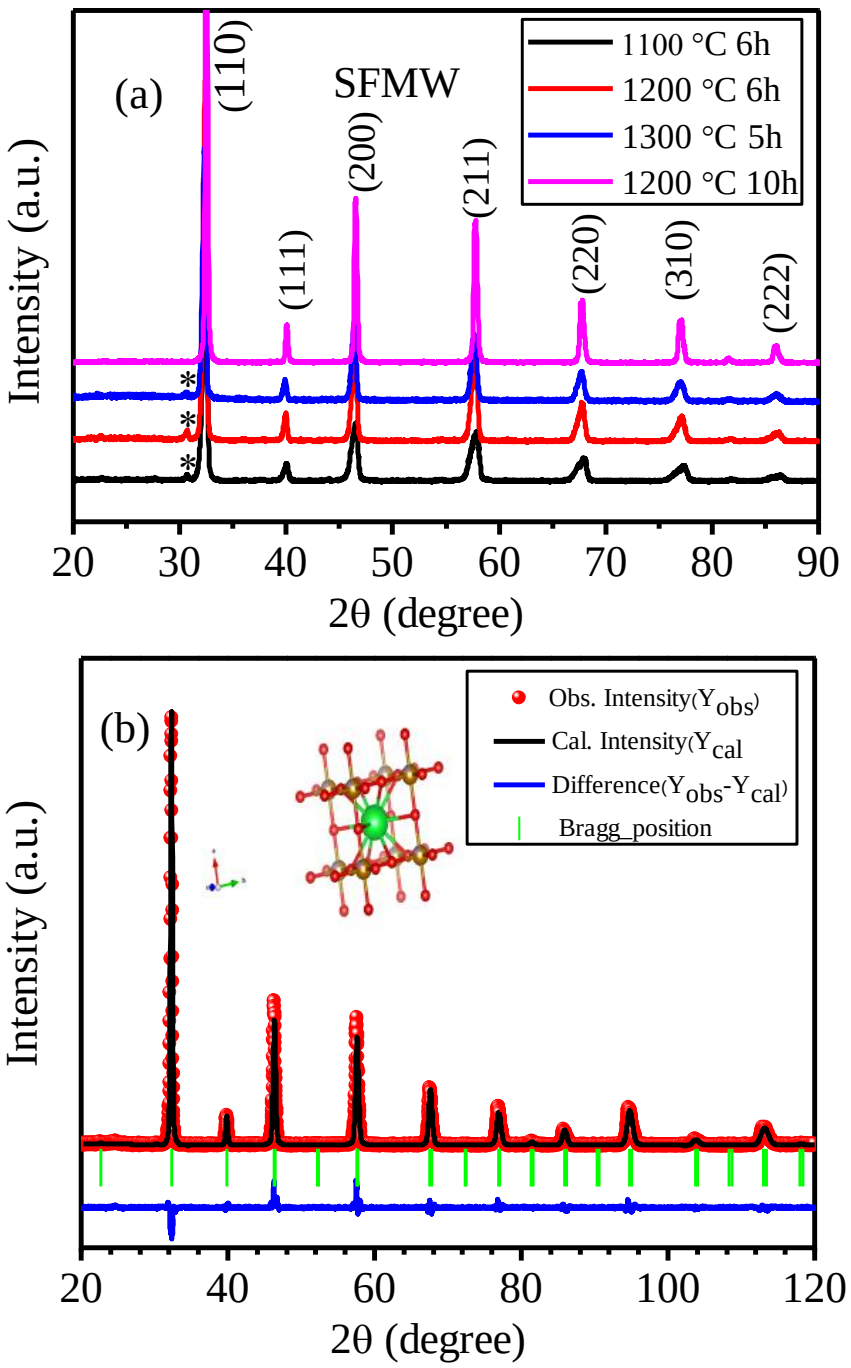

Figure 5.1 (a) Room temperature XRD patterns of the SFMW samples calcined at various temperatures and time (b) Rietveld fit for the XRD pattern of the SFMW sample at room temperature. Calculated (solid line), experimentally observed (circles), difference (bottom) and the vertical bars correspond to the permitted Bragg reflections positions.

5.3.2 Microstructure

The microstructure of the calcined and sintered samples of $SrFe_{0.8}Mo_{0.1}W_{0.1}O_3$ were analyzed by scanning electron microscopy (SEM) as presented in Figure 5.2a and 5.2b, respectively. The SEM image of calcined sample in Figure 5.2a exhibits porous, homogeneous nature as well as the good particle connectivity. These porous structures will be helpful for the oxygen ion diffusion and charge conduction from cathode side to anode. Further, no delamination and cracks are seen on the sample surface, which suggests that the materials are suitable for the cathode. Figure 5.2b present the SEM micrograph of the pellet sintered at 1200ºC for 10 hrs, which clearly indicate dense surface morphology. The sintered densities of the SFMW samples reach around 95 % of the theoretical density, implying that the sintering temperature in this study is optimum. The recorded EDX spectra of calcined and sintered SFMW sample are illustrated in Figure 5.2c and 5.2d, which confirm the presence of Sr, Fe, Mo, W, O elements close to the nominal composition within the experimental error.

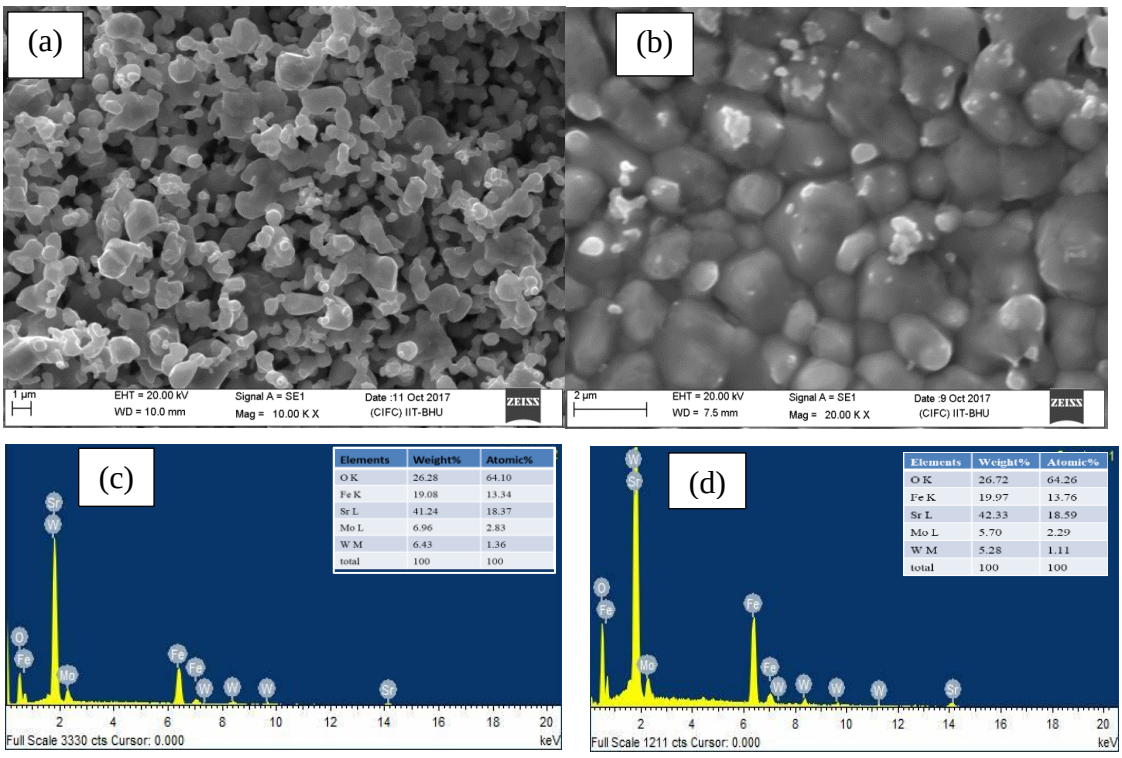

Figure 5.2 SEM and EDX images of SFMW cathode material (a-c) calcined and (b-d) sintered.

5.3.3 Chemical Compatibility with SDC and BCS Electrolytes

The chemical reaction at the interfaces of the electrode and the electrolyte is very deleterious, which increases the interfacial polarization resistance, and lead to degrade the performance of SOFCs. Hence, in present work, we investigated chemical compatibility between the prepared cathode powder samples with the electrolyte materials. The cathode SFMW powder was mixed separately with SDC ($Ce_{0.8}Sm_{0.2}O_{2-\delta,}$ oxide ion conductor electrolyte) and BCS ($Ba_{0.8}Ce_{0.1}Sn_{0.1}O_{3,}$ proton ion conductor electrolyte) powders using agate mortar-pestle and ground thoroughly using acetone as grinding medium. Then, the mixture was heat treated at 1200ºC for 6 h. Figure 5.3a and 5.3b show XRD patterns of these calcined mixtures, recorded at room temperature. All the diffraction peaks appearing in the XRD patterns of the calcined mixtures can be indexed to individual phases of SFMW/SDC and SFMW/BCS. No any additional diffraction peak of impurity caused by chemical reactions between electrode and electrolyte materials can be observed confirming that SFMW has a good chemical compatibility with SDC as well as BCS electrolytes.

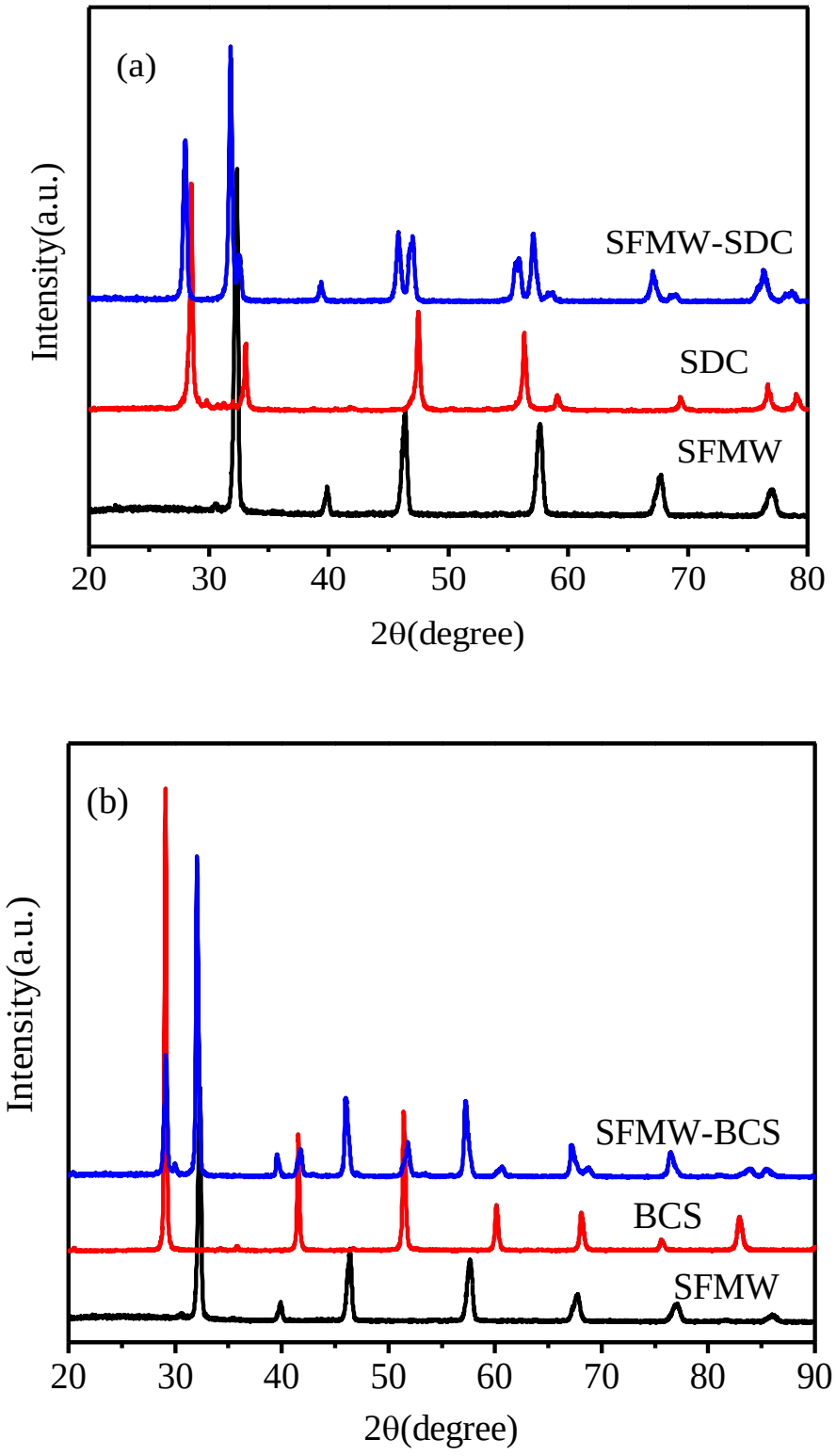

Figure 5.3 The room temperature XRD patterns of (a) SFMW-SDC and (b) SFMW-BCS mixture heat treated at 1200℃ for 6 h.

5.3.4 Thermal expansion behavior

In SOFCs, larger mismatch in the thermal expansion coefficients (TEC) of the electrode and the electrolyte materials would lead to an interior stress at the interface, persuaded throughout the thermal process, which will adversely affect the SOFCs performance. Figure 5.4a and 5.4b show the variation of lattice parameter and thermal expansion coefficient plots of the SFMW cathode from room temperature (RT) to 1000℃, characterized in air. It is not completely linear for the entire temperature region, but at around 480℃, an inflection point is observed for SFMW sample. The slope of the TEC curve is somewhat increased beyond this temperature which is associated to the release of lattice oxygen and the formation of oxygen vacancies in the SFMW in high temperature region, leading to lattice expansion. The estimated average TEC in the temperature range RT-1000℃ for SFMW, is 16×10^{-6} K^{-1}, which is lower/comparable to other cobalt-free perovskite electrode materials, such as, 30.0×10^{-6} K^{-1} for $Ba_{0.5}Sr_{0.5}Co_{0.2}Fe_{0.8}O_{3-\delta}$ [Lim et al., 2007], 20.6×10^{-6} K^{-1} for $SrFe_{0.8}Mo_{0.2}O_{3-\delta}$ [Xiao et al., 2012] and 24.5×10^{-6} K^{-1} for $Ba_{0.05}La_{0.95}FeO_{3-\delta}$ [Ding et al., 2014]. With increasing temperature, the oxygen vacancies are created as a result of loss of lattice oxygen, which in turn leads to weakening of the strength of the B–O bonds and an increase in the size of the BO_6 octahedron, causing in lattice expansion of perovskite lattice. Further, to examine the thermal stability of the samples, high temperature X-ray diffraction characterization was conducted on the SFMW powders. The XRD patterns recorded at every 100 ℃ interval is depicted in Figure 5.4c. On increasing temperature, no any phase change or appearance of secondary phases is observed except the shift in the XRD peak of the SFMW cathode sample towards the lower angle side, signifying the lattice expansion of the perovskite, as reported in many B-site double perovskite oxides [Fu et al., 2020].

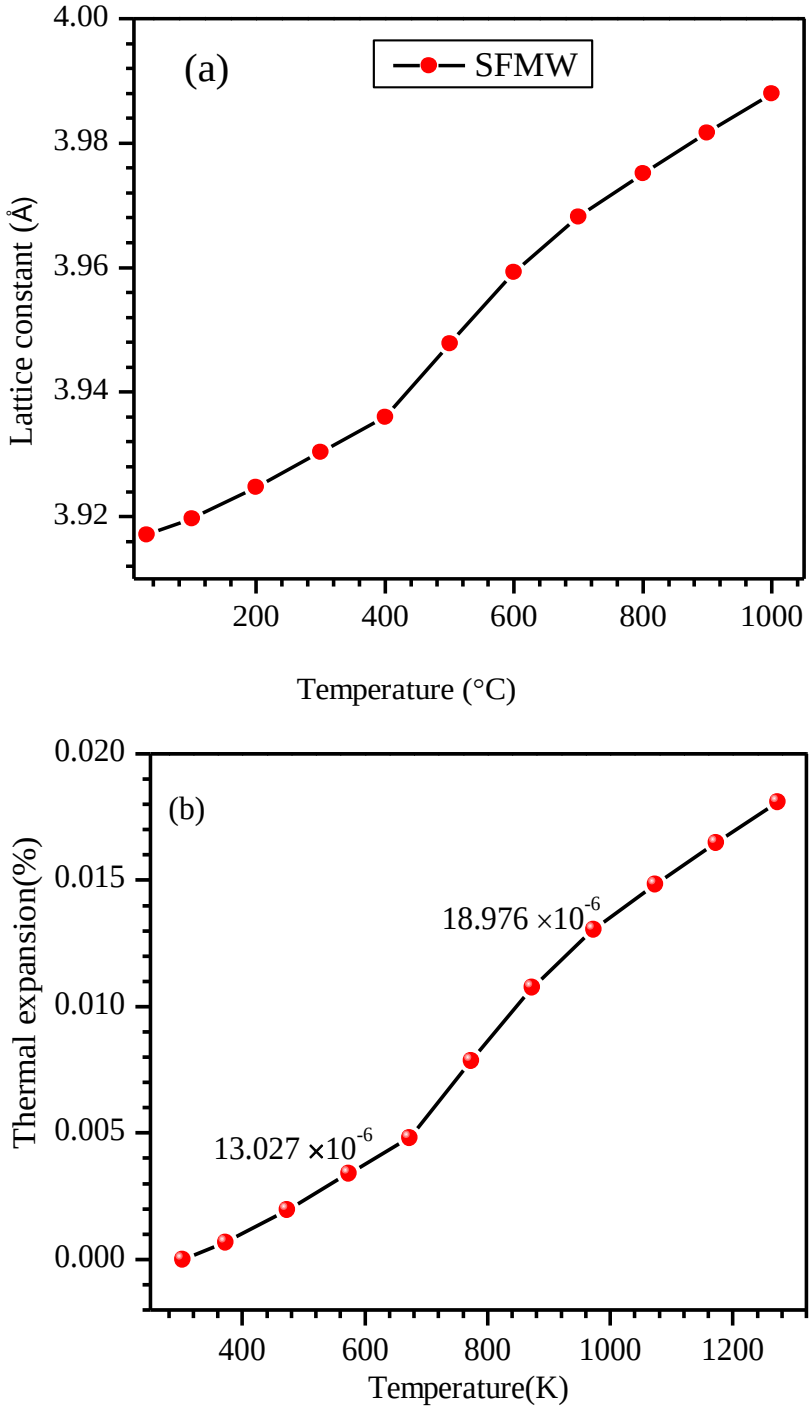

Figure 5.4 (a) Variation of lattice constant with temperature, (b) evolution of thermal expansion coefficient with temperature.

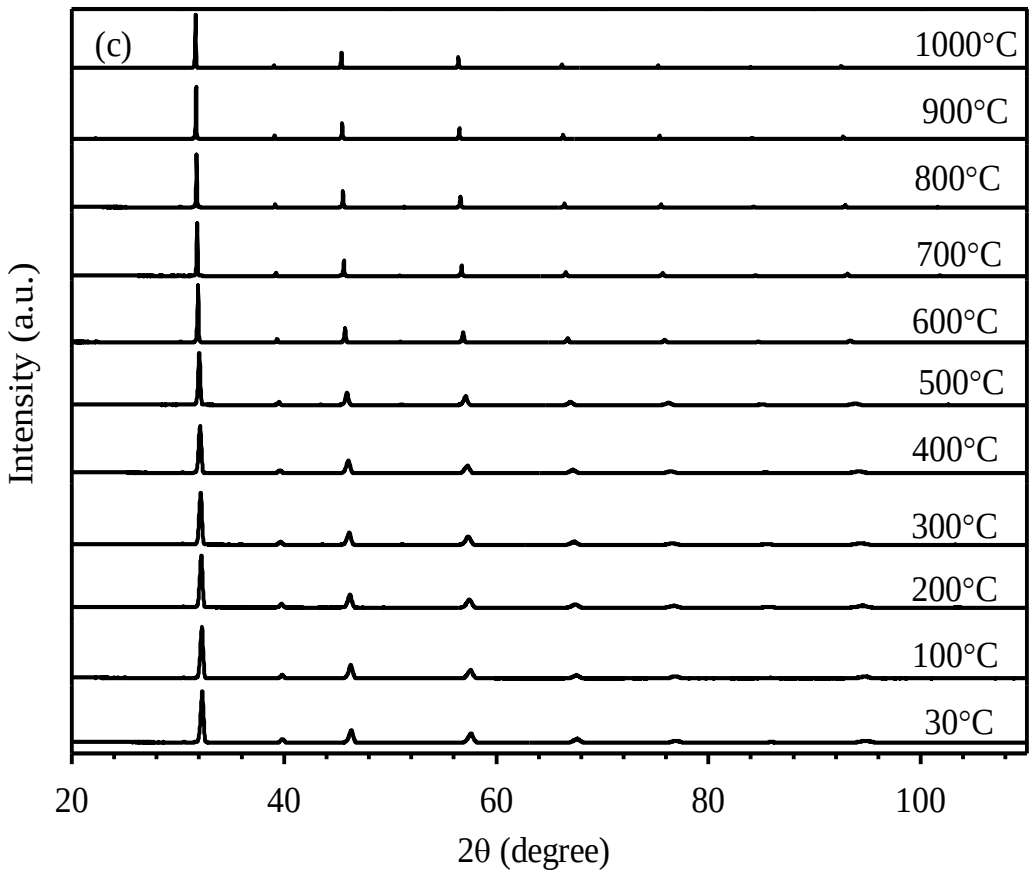

Figure 5.4 (c) Evolution of XRD patterns with temperature for SFMW sample.

In order to further minimize the mismatch of thermal expansion coefficients between cathode and electrolyte, the addition of SDC (TEC = 11.4×10^{6} K^{-1}, RT–1000ºC) electrolyte into SFM, SFW and SFMW cathode materials in (1:1 wt%) could be an effective approach. As expected, the addition of smaller TEC of SDC led to a reduction in the calculated thermal expansion coefficient value as $(14.9\pm0.2)\times10^{-6}$, $(14.4\pm0.1)\times10^{-6}$ and $(14.3\pm0.1)\times10^{-6}$ for SFM-SDC, SFW-SDC and SFMW-SDC composite cathodes, respectively. The Evolution of thermal expansion coefficient of these composite cathode materials is depicted in Figure 5.5. It can be seen that very good thermal stability is observed for all these cathode materials with nearly same thermal expansion coefficients in the entire temperature range from RT to 1000 ^{o}C.

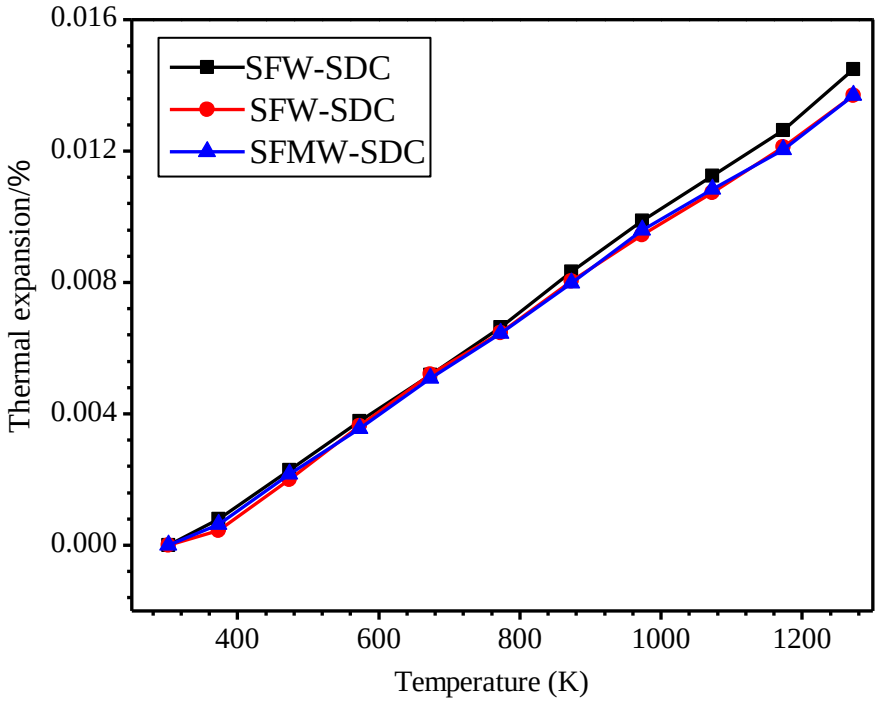

Figure 5.5 Evolution of Thermal expansion coefficient of composite cathode materials with SDC electrolyte

5.3.5 ac impedance analysis

The electrochemical characteristics of the sintered pellets of SFMW cathode was examined in temperature range 500-700℃ by the impedance spectra in the frequency range of 20Hz-5MHz. The Nyquist plot (Figure 5.6a) represents a single arc associated with grain resistance and grain boundary resistance at intermediate and lower frequencies which can best be fitted by Z-Simpwin software according to the equivalent electrical circuit $L+R_1+CPE_1/R_2+CPE_2/R_3$, as shown in the inset to Figure 5.6a, where L refers the inductance derived from electrode polarization process and measurement apparatus, and constant phase element (CPE) refers to the non-ideal capacitor. The sum of R_2 and R_3 can be attributed to the total electrode polarization resistance (R_t), demonstrating the ohmic resistance related by both ions and electrons. The total

conductivity of the cathode material was calculated by the formula $\sigma=L/R_t \times A$, where σ represents the total electrical conductivity, L represents thickness of sintered pellet, R_t represents the total ohmic resistance, and A represents the active surface area. The total electrical conductivity for the cathode sample in the temperature range 200°C to 700°C are fitted by the Arrhenius plot as shown in Figure 5.6b. The activation energy was obtained from the slope of the plot by applying the Arrhenius equation: $\sigma_t = (\sigma_o/T) \exp(-E_a/ k_B T)$. Here, σ_o is the pre-exponential factor, E_a is the activation energy, T stands for absolute temperature, and k_B is the Boltzmann constant. The activation energy E_a for SFMW sample is found to be 0.32 eV. For oxide ion conduction, the value of E_a is usually near to 1 eV and for electronic conduction, it is close to 0.1 eV. Thus having intermediate values for mixed charge conduction regimes suggest mixed ionic-electronic conduction for SFMW [Knauth et al.,2002; Xie et al.,1999; Koc et al.,1992]. According to earlier studies, the value of electrical conductivity of $SrFeO_3$ is influenced by partial pressure of oxygen and oxygen content, and the p-type conduction behavior is observed while oxygen partial pressures is above 10^{-5} atm. Therefore, SFMW sample studied in air should exhibit the p-type conduction behavior [Zhu et al., 2017]. Meanwhile, thermal reduction of ion resulting the formation of oxygen vacancies which confirm the oxygen-ionic conductivity in SFMW. Thus, it is a mixed oxygen ion and electron conductor but having predominant p-type conducting behavior.

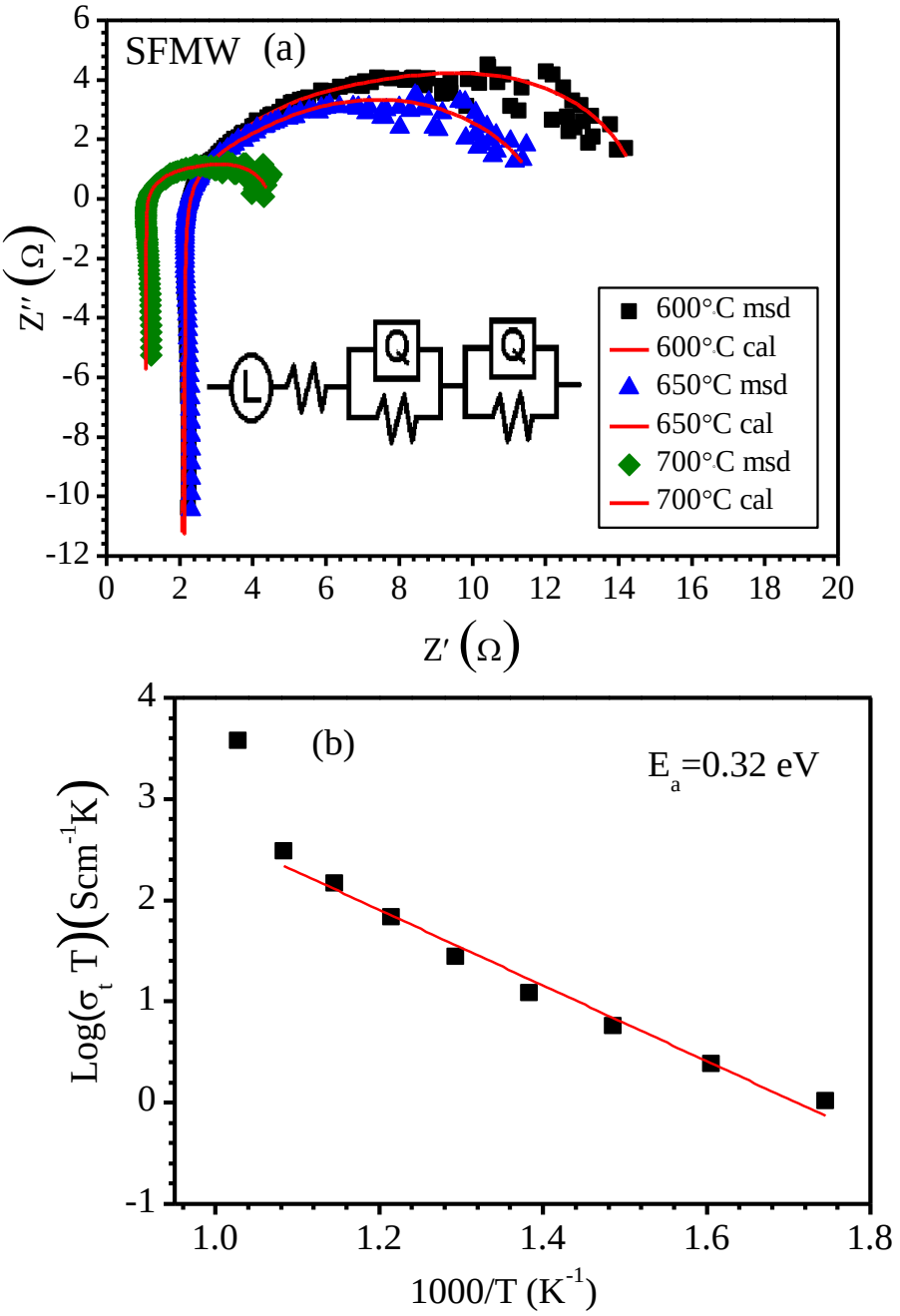

Figure 5.6 (a) Impedance spectra of SFMW cathode (b) Arrhenius conductivity-temperature plot of SFMW cathode sample.

5.3.6 Electrochemical performance of single cell

Electrochemical performance of the cobalt free SFMW cathode was examined in the temperature range 600-700ºC by the impedance spectra as presented in Figure 5.7a. The impedance spectra consist one semicircle arcs and a long tail located at

low to intermediate frequency and high frequency regions, respectively. In order to obtain the value of area specific resistance(ASR), Nyquist plots were fitted by the least square fitting method (Z-Simpwin software), with an equivalent circuit (inset to Figure 5.7a) containing one inductor L, one Re_l resistance and two parallel associated in series of R//CPE elements. In this equivalent electrical circuit, Re_l could be allocated to the ohmic resistance (R_{ohm}) from the intercept value with the real axis at high frequency side. The constant phase elements assigned as CPE_1 and CPE_2 whose values reveal the reaction mechanism of various electrode processes. The resistance evaluated through depressed arcs are associated to the electrode process such as a resistance originated through ion charge transfer process (R_1, the size of intermediate-frequency arc), and a resistance originated through surface diffusion of oxygen specimen and mass transfer process (R_2, the size of low frequency arc) [Yang et al., 2016]. The total electrode polarization resistance (R_p) is the sum of R_1 and R_2. As expected, an increase of the measurement temperature leads to a considerable reduction of the Area specific resistance (ASR) calculated by using formula $ASR=R_p \times A/2$, where A stands for active surface area. The values of ASR of SFMW cathode are 1.65, 4.2 and 9.75 Ω-cm^2 at 700, 650 and 600ºC respectively measured in air. A plot of ln (ASR) versus 1000/T is shown in Figure 5.7b. The slope of linear fit of this was used to calculate the value of activation energy (E_a) of the symmetrical cell. The value of E_a for cobalt–free SFMW single cell corresponding to the SDC electrolyte is 1.13eV which is smaller/comparable to the earlier reported values of 1.20, 1.25, 1.26, 1.20, and 1.15 eV for other cobalt-free cathodes $Pr_{0.5}Sr_{0.5}Fe_{0.8}Cu_{0.2}O_{3-\delta}$, $Nd_{0.5}Sr_{0.5}Fe_{0.8}Cu_{0.2}O_{3-\delta}$, $Ba_{0.95}Ca_{0.05}FeO_{3-\delta}$, $Sm_{0.5}Sr_{0.5}Fe_{0.8}Cu_{0.2}O_{3-\delta}$, and $Gd_{0.5}Sr_{0.5}Fe_{0.8}Cu_{0.2}O_{3-\delta}$ respectively [Fu et al., 2020].

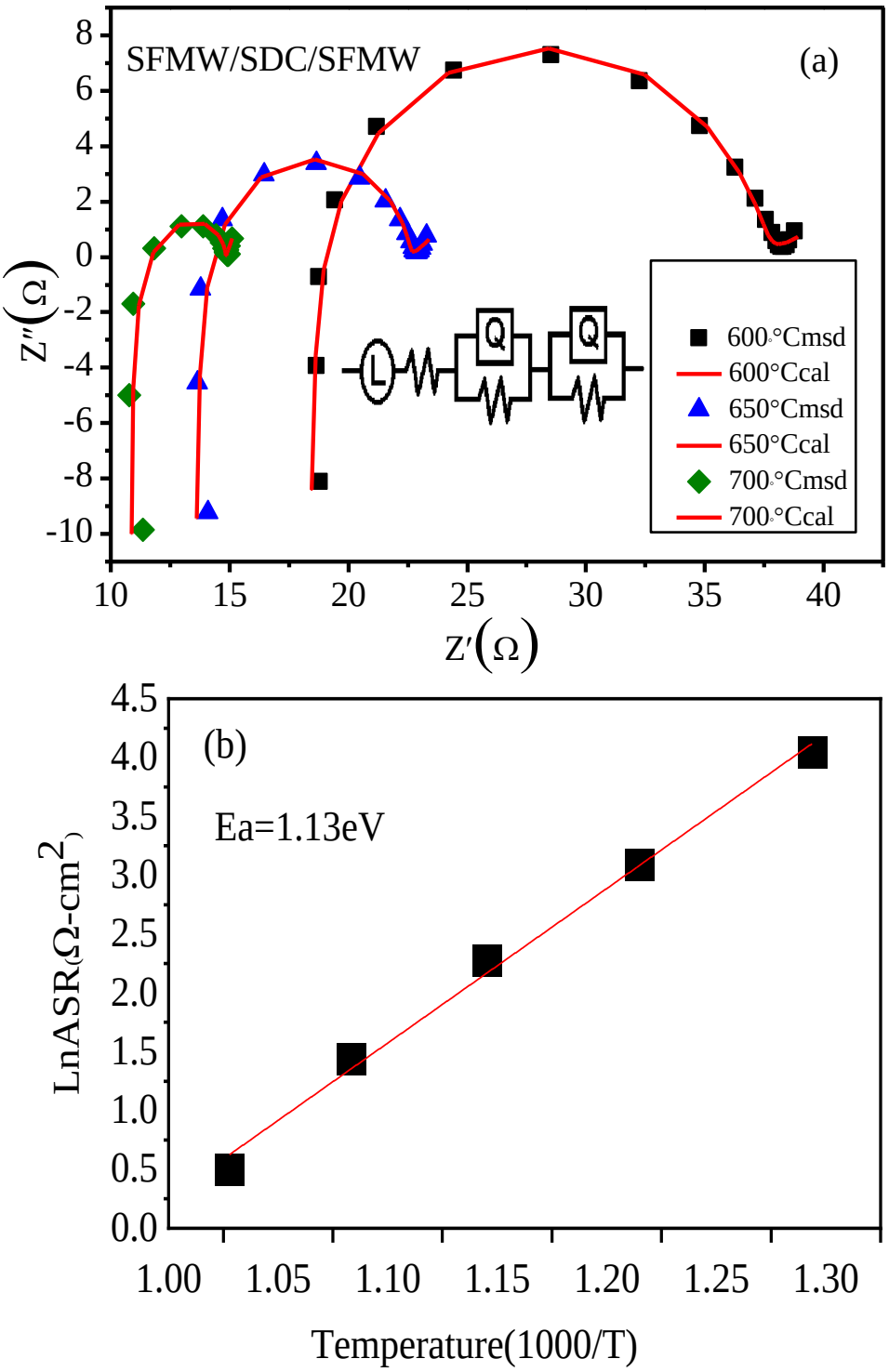

Figure 5.7 (a) Impedance spectra of single cell of SFMW cathode corresponding to the oxide ion conductor SDC electrolyte. (b) Arrhenius plot of the ASRs of SFMW/SDC/SFMW cathode.

The SEM image of the interface of the SFMW cathode and the SDC electrolyte is presented in Figure 5.7c and 5.7d. The layer of porous cathode having thickness 100μm is seen to adhere rigidly to the electrolyte without apparent cracks and defects indicating the thermal compatibility between these two cell components.

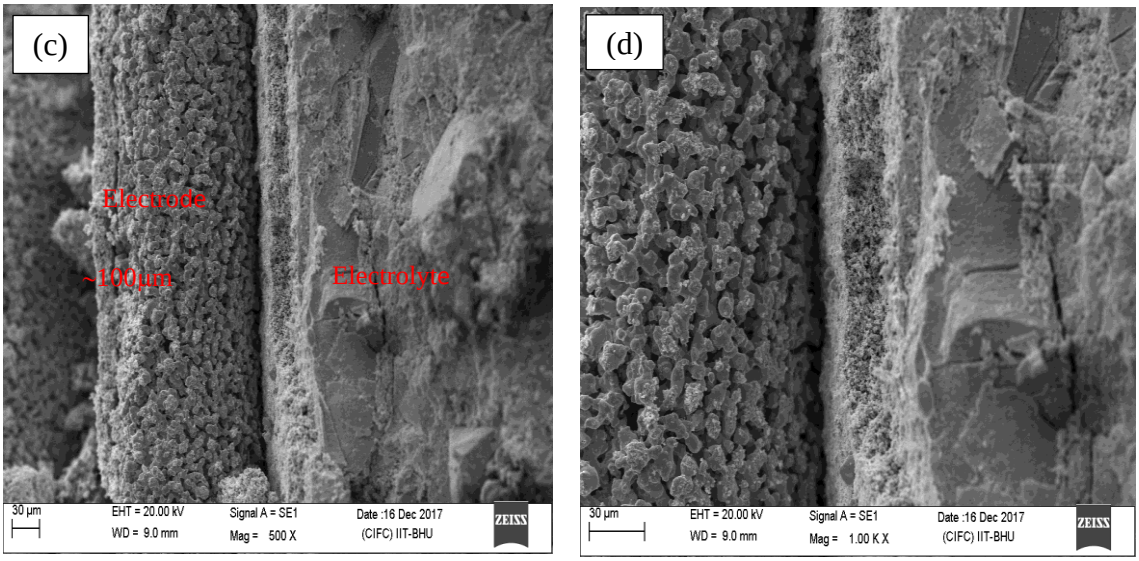

Figure 5.7 (c, d) SEM images of cross section of SFMW/SDC/SFMW interface

5.4 Conclusions

In summary, Cobalt-free $SrFe_{0.8}Mo_{0.1}W_{0.1}O_3$ perovskite oxide was synthesized via industrially viable high energy ball milling technique and its cubic crystal structure with P*m-3m* space group was confirmed using X-ray powder diffractometer. It is shown that SFMW has a good chemical compatibility with SDC as well as BCS electrolytes even after heat treatment at 1200ºC for 6h, as characterized by XRD measurement. The average TEC of SFMW sample is 16×10^{-6} K^{-1} for the temperature range RT to 1000ºC. The activation energy E_a for SFMW sample is found to be 0.32 eV which suggests the existence of mixed ionic-electronic conductivity in the material. The ASR value of the SDC electrolyte supported symmetrical cell is 1.65 Ω-cm^2 at 700ºC in air under open-circuit conditions. Thus, we can conclude from present research work that, SFMW prepared by a co-doping approach is a promising cathode material for SOFCs.